Angular Momentum and Temperature Homogenization in the Symmetric Circulation of the Atmosphere

PAOLA CESSI*

Scripps Institution of Oceanography, La Jolla, California

(Manuscript received 10 February 1997, in final form 30 September 1997)

ABSTRACT

The axisymmetric model of the Hadley circulation can be systematically reduced in the limit of small Rossby number to a simpler one-dimensional system. The reduced system governs the nonlinear evolution of the surface angular momentum and the vertically averaged potential temperature. The meridional transports of heat and angular momentum take the form of downgradient nonlinear diffusion, which acts to homogenize laterally the angular momentum and the potential temperature within the meridional Hadley cells. The diffusivities for both quantities are proportional to the square of the latitudinal gradient of potential temperature. The reduced system is amenable to analytic exploration and allows the explicit determination of the extent and strength of the meridional circulation in terms of the parameters of the problem, such as the Rossby number, the stratification imposed by the radiative–convective equilibrium, and the surface drag. The reduced system also shows that surface easterlies at the equator are possible even when the heating distribution is latitudinally symmetric, as long as the surface drag or the imposed stratification are small.

1. Introduction

That the meridional thermal contrast produced by radiative–convective equilibrium can produce a meridional circulation on a rapidly rotating planet like the earth is not at all obvious: a zonal wind in cyclostrophic balance is a solution of the equations of motions in the inviscid case. However, such a solution, with no meridional circulation, is untenable in the presence of friction.

The role of friction in symmetric models of the Hadley circulation is a contradictory one. On one hand, Ekman layers are the site at which the thermal wind balance is broken and a meridional circulation, down the pressure gradient, is allowed (Charney 1973). This frictionally driven flow results in a meridional cell, and theoretical ideas usually appeal to conservation of angular momentum in order to explain the cell properties and the associated surface zonal winds (Schneider 1977; Held and Hou 1980). Thus nonzero friction is required for the existence of the meridional flow, but angular momentum conservation is supposed not to be upset by friction.

The constraints imposed by quasi conservation of angular momentum are strong and lead to well-accepted scaling arguments for the extent of the meridional cell (Lindzen 1990). However, in order to make quantitative estimates beyond the scaling laws, the precise functional relationship between streamfunction and angular momentum must be determined. This is a difficult task in the present context because

1) all the streamlines are closed and there is no ''upstream region'' where the dependence of the angular momentum on the streamfunction is set by external processes
2) according to the numerical calculations presented in the published literature, all the streamlines pass through a viscous boundary layer forbidding application of the Prandtl–Batchelor theorem.

One hypothesis is that the meridional circulation acts as a vigorous blender so that angular momentum is approximately homogenized (Bretherton and Turner 1968; Fang and Tung 1996). While appealing, this scenario has not been deductively demonstrated, and its limits of validity (if any) have not been established.

In the following we examine a regime that attempts to bridge the gap between frictionally dominated linear dynamics and a quasi-inviscid, fully nonlinear flow. The meridional flow is assumed to be weak as in Charney's linear model, but advection of angular momentum and potential temperature by the meridional circulation is included. Despite the weakness of the meridional flow, the streamlines are approximately coincident with the lines of constant angular momentum and potential tem-

* Additional affiliation: Instituto FISBAT–CNR, Bologna, Italy.

Corresponding author address: Dr. Paola Cessi, Scripps Institution of Oceanography, UCSD-0230, La Jolla, CA 92093-0230.
E-mail: cessi@hank.ucsd.edu

perature, except in thin Ekman layers. We show that, in all parameter ranges, the circulation homogenizes laterally the potential temperature within the bulk of the meridional circulation. Thus the thermal gradients imposed by the radiative–convective heating are greatly reduced. In the parameter range where the circulation becomes very vigorous, both in the meridional and zonal directions, the angular momentum is also homogenized.

2. Nondimensionalization and conservation laws

Our point of departure is the symmetric model used by Charney (1973) in the limit of a thin spherical shell. If a is the radius of the sphere, φ is the latitude, and

$$y \equiv a \sin\varphi, \qquad c(y) \equiv \cos\varphi = \sqrt{1 - y^2/a^2}, \quad (2.1)$$

then the zonal momentum equation can be written in the form

$$u_t + J(\psi, u) + \psi_z c^{-1}[2\Omega a^{-1} y + a^{-2}c^{-1}yu] = \nu_V u_{zz} + \nu_H[2a^{-2}u + c(cu)_{yy}]. \quad (2.2)$$

In (2.2) ψ is the meridional streamfunction defined by

$$\partial_y \psi \equiv w, \qquad \partial_z \psi \equiv -cv, \quad (2.3)$$

and the Jacobian is $J(A, B) = A_y B_z - A_z B_y$.

The right-hand side of (2.2) contains anisotropic viscosity. Apart from the anisotropy these dissipative terms have been constructed by analogy molecular processes. Thus, the horizontal viscosity ν_H mixes the rotation rate $\omega = \Omega + u/(ac)$ so that there are no viscous stresses if the atmosphere is in solid-body rotation (e.g., Read 1986). If the viscosity is isotropic (i.e., if $\nu_H = \nu_V$), then the term proportional to ν_H in (2.2) will be much less than the term proportional to ν_V in the thin shell limit. This is why the formulations of Schneider (1977) and Held and Hou (1980, HH hereafter) do not include horizontal viscosity. However, our results suggest that if $\nu_H = 0$ then (2.2) is ill-posed: singularities are not surprising since there is nothing that prevents u from becoming discontinuous in y. If $\nu_H \neq 0$ these discontinuities can be smoothed by lateral boundary layers.

Instead of the zonal momentum u we will use the angular momentum

$$M \equiv \Omega a c^2 + uc \quad (2.4)$$

as a dependent variable. Rewriting (2.2) in terms of M produces the more transparent conservation equation

$$M_t + J(\psi, M) = \nu_V M_{zz} + \nu_H[c^4(c^{-2}M)_y]_y. \quad (2.5)$$

The meridional momentum equation and the hydrostatic relation are combined into a single equation for the zonal vorticity, which in the thin shell approximation reads

$$(c^{-2}\psi_{zz})_t + J(\psi, c^{-2}\psi_{zz}) - a^{-2}c^{-4}y(M^2)_z = \frac{g}{\theta_0}\theta_y + \nu_V c^{-2}\psi_{zzzz} + \nu_H \psi_{zzyy}. \quad (2.6)$$

Once again, the last term in (2.6) is negligible when $\nu_H = \nu_V$ except in lateral boundary layers. Again, the lateral friction tends to homogenize the zonal rotation rate, ψ_{zz}, rather than the zonal vorticity, $c^{-2}\psi_{zz}$.

Finally, the potential temperature evolves according to

$$\theta_t + J(\psi, \theta) = \nu_V \theta_{zz} + \nu_H(c^2\theta_y)_y + \tau^{-1}(\theta_E - \theta), \quad (2.7)$$

where τ is the relaxation time toward the radiative–convective equilibrium distribution $\theta_E(y, z)$.

A stress-free, no-flux rigid lid is assumed at the top of the spherical shell; that is,

$$\psi = M_z = \psi_{zz} = \theta_z = 0, \quad \text{at} \quad z = H. \quad (2.8)$$

At the rigid bottom the stress is parametrized by a drag-type law, linearized around constant velocity, and a no-flux condition is imposed on the potential temperature:

$$\nu_V M_z = C(M - \Omega a c^2), \qquad \nu_V \psi_{zz} = C\psi_z, \qquad \psi = \theta_z = 0, \quad \text{at } z = 0. \quad (2.9)$$

The bottom drag relaxes the angular momentum M to the local planetary value $\Omega a c^2$.

As in HH, it is assumed that the radiative–convective equilibrium temperature distribution θ_E is of the form

$$\theta_E/\theta_0 = \Delta_V(z/H - 1/2) + \Delta_H \Theta_E(y). \quad (2.10)$$

The system (2.5) through (2.9) is nondimensionalized using a scaling that follows that of Schneider and Lindzen (1977), except that the zonal velocity u is implicitly scaled with Ωa:

$$(z, y) = a(\epsilon\hat{z}, \hat{y}), \qquad M = \Omega a \hat{M}, \qquad \theta = \theta_0 \Delta_H \hat{\theta}, \qquad \psi = \nu_V R \epsilon^{-1}\hat{\psi}, \qquad t = (RE\Omega)^{-1}\hat{t}. \quad (2.11)$$

We have used a standard notation for the thermal Rossby number R, the Ekman number E, and the aspect ratio ϵ, defined as

$$R \equiv gH\Delta_H/(\Omega^2 a^2), \qquad E \equiv \nu_V/(\Omega H^2), \qquad \epsilon \equiv H/a. \quad (2.12)$$

The viscous scaling in (2.11) for the streamfunction is imposed by the Ekman balance responsible for the meridional circulation: a meridional Ekman transport is generated to the left of the geostrophically balanced vertical shear. In turn the vertical shear of the zonal flow is in thermal wind balance.

Dropping the carets from now on, the nondimensional equations for the angular momentum, zonal vorticity, and potential temperature are

$$R[M_t + J(\psi, M)] = M_{zz} + \mu[c^4(c^{-2}M)_y]_y,$$

$$R^2E^2[c^{-2}\psi_{zzt} + J(\psi, c^{-2}\psi_{zz})] - yc^{-4}(M^2)_z = R\theta_y + RE^2[c^{-2}\psi_{zzzz} + \mu\psi_{zzyy}],$$

$$R[\theta_t + J(\psi, \theta)] = \theta_{zz} + \mu[c^2\theta_y]_y + \alpha[\Theta_E(y) + \Delta(z - 1/2) - \theta]. \quad (2.13a,b,c)$$

The nondimensional boundary conditions are

$$M_z = \gamma(M - c^2), \qquad \psi_{zz} = \gamma\psi_z,$$
$$\psi = \theta_z = 0 \qquad \text{at } z = 0,$$
$$M_z = \psi_{zz} = \psi = \theta_z = 0 \quad \text{at } z = 1. \tag{2.14}$$

Thus, in addition to the three parameters defined in (2.12), there are four more parameters:

$$\alpha \equiv H^2/(\tau\nu_V), \qquad \Delta \equiv \Delta_V/\Delta_H, \qquad \gamma \equiv CH/\nu_V,$$
$$\mu \equiv \epsilon^2\nu_H/\nu_V. \tag{2.15}$$

Here α is the ratio of the viscous timescale across the depth of the model atmosphere to the relaxation time toward the radiative–convective equilibrium; Δ measures the prescribed stratification in the absence of circulation; γ is the ratio of the spindown time due to the drag to the viscous timescale, and μ measures the ratio of the horizontal to the vertical viscosity.

With the scaling (2.11), the Ekman number appears only in the zonal vorticity equation (2.13b), while the frictional and diffusive terms in the angular momentum and potential temperature equations are as large as the inertial terms. This is not surprising because in a symmetric model the meridional circulation is all generated inside viscous boundary layers.

In summary there are six nondimensional parameters, R, E, α, Δ, γ, μ, and one externally prescribed latitudinal distribution of temperature, $\Theta_E(y)$.

3. Asymptotic reduction in the small Rossby number limit

In the limit of small Rossby number R, it is possible to obtain an expansion that reduces the system (2.13) to a simpler set of equations. There is a distinguished limit in which the parameters are ordered with respect to $R \ll 1$. Specifically we take $R \to 0$ with

$$\mu = R^2\mu_2, \quad \gamma = R^2\gamma_2, \quad \alpha = R^2\alpha_2, \quad \Delta = R^{-1}N^2. \tag{3.1}$$

The smallness of α and γ should not be interpreted as a requirement that the vertical viscosity ν_V is large; rather, it is a statement about the slowness of the radiative processes, τ, and of the surface drag. The importance of viscosity is measured by the Ekman number, which is assumed to be small.

The distinguished limit (3.1) is suggested by the balance obtained integrating (2.13a) and (2.13c) vertically:

$$R[\overline{M}_t + (\overline{\psi M_z})_y] = -\gamma[M(y, 0, t) - c^2] + \mu[c^4(c^{-2}\overline{M})_y]_y,$$
$$R[\overline{\theta}_t + (\overline{\psi\theta_z})_y] = \mu[c^2\overline{\theta}_y]_y + \alpha[\Theta_E(y) - \overline{\theta}], \tag{3.2a,b}$$

where the overbar indicates the vertical average.

Neglecting lateral dissipation, (3.2a) shows that the surface zonal wind, proportional to the difference between the surface angular momentum $M(y, 0, t)$ and its planetary value, is given by the meridional transport of vertical shear. If the vertical shear M_z is in approximate thermal wind balance, then $M_z = O(R)$, and the meridional flux of angular momentum $R(\overline{\psi M_z})_y$ is $O(R^2)$. The choice $\gamma = O(R^2)$ on the right-hand side of (3.2a) guarantees a fair competition between advection, which makes angular momentum constant along streamlines, and bottom drag, which injects gradients in the surface angular momentum. Also with $\mu = O(R^2)$ and $\partial_t = O(R)$ all the terms in (3.2a) have the same asymptotic order, namely, $O(R^2)$.

Similarly, (3.2b) indicates that the lateral redistribution of vertically averaged equilibrium temperature is accomplished through the meridional transport of temperature that departs from the vertical average, that is, the term $R(\overline{\psi\theta_z})_y$. If the imposed stratification Δ vanishes, then the stratification driven by the meridional circulation is $O(R)$, and its meridional transport is $O(R^2)$. The choice $\alpha = O(R^2)$ allows a fair competition between advective and radiative processes in establishing the temperature distribution. Given this scaling, Δ must be $O(R^{-1})$ in order to contribute to the vertical stratification as much as advection.

It is possible that other parameters orderings lead to interesting balances. The one selected here allows us to include many dynamical processes in the balance while being amenable to analytic exploration. Balances involving fewer processes are recovered on considering special limits of the final evolution equations.

Remarkably, as we will show in section 4, the distinguished limit (3.1), leads to quantitative agreement with the numerical solutions of (2.13) published in the literature, even when α_2 and γ_2 are large.

Although we will be mainly concerned with the steady circulation, the asymptotic reduction detailed below can be applied also to time-dependent flows whose timescale of evolution is slow; that is, $\partial_t = R\partial_{t_1}$. With this choice, an expansion is possible in which M, θ, and ψ are expanded in powers of R; that is,

$$(M, \theta, \psi) = (M_0, \theta_0, \psi_0) + R(M_1, \theta_1, \psi_1) + R^2(M_2, \theta_2, \psi_2) + \cdots. \tag{3.3}$$

a. The $O(R^0)$ balance

The terms of $O(R^0)$ in the system (2.13) are

$$0 = M_{0zz},$$
$$-yc^{-4}(M_0^2)_z = 0$$
$$0 = \theta_{0zz}. \tag{3.4}$$

At this order both the top and bottom boundary conditions are $M_{0z} = \theta_{0z} = 0$. Thus the solution of (3.4) is

$$M_0 = \mathcal{M}(y, t_1), \qquad \theta_0 = \Theta(y, t_1). \tag{3.5}$$

To a first approximation, the angular momentum and

the potential temperature are independent of height but are undetermined at this order. It will be apparent at next order that, even though the leading order balance is viscous and diffusive, the vertically uniform fields in (3.5) are also exact solutions when the nonlinear terms are included. Our goal is to find the evolution equations for $\mathcal{M}$ and Θ.

b. The O(R) balance

At the next order, we have from (2.13):

$$J(\psi_0, M_0) = M_{1zz},$$
$$-2yM_0M_{1z} = c^4\theta_{0y} + E^2c^2\psi_{0zzzz},$$
$$J(\psi_0, \theta_0) = \theta_{1zz} + \alpha_2N^2(z - 1/2). \quad (3.6a,b,c)$$

Although the last term in (3.6b) is negligible if $E \ll 1$, it is not so uniformly in height, and it is kept at this order. The solution of (3.6), which satisfies the no-flux and no-stress conditions at the top and bottom, is

$$M_{1z} = -\psi_0\mathcal{M}_y,$$
$$\psi_0 = -\Theta_y\phi(z, y, \mathcal{M}),$$
$$\theta_{1z} = \frac{1}{2}\alpha_2N^2z(1 - z) + \Theta_y^2\phi(z, y, \mathcal{M}). \quad (3.7a,b,c)$$

The meridional circulation, characterized to a first approximation by ψ_0, depends on the yet unknown latitudinal temperature gradient Θ_y, which is not necessarily clamped to that imposed by the radiative–convective equilibrium Θ_E. In (3.7) we have introduced the variable ϕ, which is defined to be the solution of the ordinary differential equation

$$E^2c^2\phi_{zzzz} - y(\mathcal{M}^2)_y\phi = c^4, \quad (3.8)$$

with boundary conditions $\phi = \phi_{zz} = 0$ at $z = 0, 1$. The explicit expression for ϕ is somewhat complicated and is given in appendix A: it is a nonlinear version of Charney's (1973) solution with an Ekman boundary layer thickness proportional to $[-y(\mathcal{M}^2)_y/(cE)^2]^{-1/4}$, instead of $(4y^2/E^2)^{-1/4}$.

If the rotation rate, proportional to y on the sphere, vanishes, then ϕ, the solution of (3.8), becomes very large, of order E^{-2}; that is, ϕ obeys the nonrotating balance. Because the actual meridional circulation, given in (3.7b), is proportional to the temperature gradient Θ_y as well as to ϕ, we expect a vigorous circulation unless the thermal gradient becomes small near the equator. Notice that the nonrotating behavior is also obtained if the angular momentum $\mathcal{M}$ is homogenized laterally. Thus, at least as far as the meridional circulation is concerned, angular momentum homogenization is equivalent to a weakening of the rotation.

In the inviscid limit, $E \ll 1$, the streamfunction, ψ_0 in (3.7b), is independent of height, outside the thin top and bottom boundary layers. Thus the zeroth-order angular momentum and temperature, $\mathcal{M}$ and Θ, which are also depth independent, are exact nonlinear solutions in the interior region; that is,

$$J(\psi_0, \mathcal{M}) = 0, \qquad J(\psi_0, \Theta) = 0 \quad (3.9)$$

except in the top and bottom Ekman layers. In this sense, the solutions (3.5), although springing from a viscously dominated balance, also satisfy an advectively dominated balance in the interior. Remarkably, with the scaling (3.1), the exact nonlinear solutions $\mathcal{M}(y, t_1)$ and $\Theta(y, t_1)$ automatically satisfy the zero-order boundary conditions at the top and the bottom. Therefore, the angular momentum and the potential temperature do not need boundary layer corrections at $z = 0$ and $z = 1$. This makes the derivation of the evolution equations for $\mathcal{M}$ and Θ very simple.

In this expansion the vertical stratification, θ_{1z} in (3.7c), is $O(R)$ and is determined by two terms. The first one, proportional to N^2, is a familiar one: it arises from a balance between vertical diffusion and the stratification imposed by the radiative equilibrium. The second term on the right-hand side of (3.7c) is ''dynamically driven'' stratification: the shear of the meridional velocity tilts the isotherms from their vertical position until arrested by vertical diffusion. In this way differential advection by the meridional velocity turns *horizontal* temperature gradients into *vertical* temperature gradients. Because the strength of the meridional overturning is itself proportional to the latitudinal temperature gradient, the dynamically driven stratification depends on the *horizontal temperature gradient squared.* Thus the dynamically driven stratification is always stable.

In a similar way the zonal shear, M_{1z} in (3.7a), is generated by shear tilting the lines of constant $\mathcal{M}$ from the vertical position. The constraint that the zonal shear is in cyclostrophic balance, outside the Ekman layers, determines the meridional circulation in the interior.

To obtain the $O(R)$ angular momentum and temperature corrections, M_1 and θ_1, (3.7a,c) must be integrated further in z. The additional boundary conditions necessary for the integration are arbitrary, and here they are chosen to be $M_1|_{z=0} = 0$ and $\int_0^1 \theta_1\, dz = 0$. Thus $\mathcal{M}$ is normalized to be the surface angular momentum, and Θ is the vertically averaged potential temperature. With this choice of gauge the bottom boundary condition for the angular momentum becomes $M_z = R^2\gamma_2(\mathcal{M} - c^2)$.

c. The O(R²) balance

The $O(R^2)$ angular momentum and potential temperature equations are

$$\mathcal{M}_{t_1} + (\psi_0M_{1z})_y - (\psi_0M_{1y} + \psi_1\mathcal{M}_y)_z = M_{2zz} + \mu_2[c^4(c^{-2}\mathcal{M})_y]_y,$$
$$\Theta_{t_1} + (\psi_0\theta_{1z})_y - (\psi_0\theta_{1y} + \psi_1\Theta_y)_z = \theta_{2zz} + \alpha_2(\Theta_E - \Theta) + \mu_2[c^2\Theta_y]_y, \quad (3.10)$$

with boundary conditions $\theta_{2z}|_{z=0,1} = M_{2z}|_{z=1} = 0$ and $M_{2z}|_{z=0} = \gamma_2(\mathcal{M} - c^2)$. The equations in (3.10) have a ''solvability condition,'' which is obtained by integrating vertically over the whole depth:

$$\mathcal{M}_{t_1} = \gamma_2(c^2 - \mathcal{M}) + \left[\mathcal{M}_y\Theta_y^2\int_0^1 \phi^2\, dz + \mu_2 c^4(c^{-2}\mathcal{M})_y\right]_y,$$

$$\Theta_{t_1} = \alpha_2(\Theta_E - \Theta) + \left[\Theta_y^3\int_0^1 \phi^2\, dz + \frac{1}{2}\alpha_2 N^2\Theta_y \times \int_0^1 z(1-z)\phi\, dz + \mu_2 c^2\Theta_y\right]_y. \tag{3.11}$$

The parameter μ_2, which corresponds to horizontal viscosity, can be much less than one but it is necessary to retain this process in order to obtain solutions that are regular everywhere.

In appendix A approximate expressions for the integrals involving $\phi(z, y, \mathcal{M})$ are given. Using these approximations, (3.11) becomes

$$\mathcal{M}_{t_1} = \gamma_2(c^2 - \mathcal{M}) + [F^2\Theta_y^2\mathcal{M}_y + \mu_2 c^4(c^{-2}\mathcal{M})_y]_y,$$

$$\Theta_{t_1} = \alpha_2(\Theta_E - \Theta) + [F^2\Theta_y^3 + \lambda F\alpha_2 N^2\Theta_y + \mu_2 c^2\Theta_y]_y,$$

$$F \equiv \frac{2\sqrt{2}\,\pi^{-1}c^2}{[\pi^4E^2 - yc^{-2}(\mathcal{M}^2)_y]}, \qquad \lambda \equiv 2\sqrt{2}\,\pi^{-3}. \tag{3.12a,b}$$

Thus, in this weakly nonlinear expansion, the advection of angular momentum takes the form of downgradient lateral diffusion of $\mathcal{M}$ with a ''diffusion'' coefficient, $F^2\Theta_y^2$, that is always positive and proportional to the square of the meridional temperature gradient. The role of the meridional momentum transport is indeed to homogenize the angular momentum, while the viscosity tends to homogenize the rotation rate, and the bottom drag brings the angular momentum toward the planetary value, c^2. Thus in (3.12a) there is a competition between homogenization of rotation rate, homogenization of angular momentum, and relaxation toward the planetary rotation rate.

The meridional advection of potential temperature produces an analogous term in (3.12b) proportional to the cube of the meridional temperature gradient, as well as a quasi-linear term where the diffusivity is proportional to the imposed stratification N^2: if the imposed stratification is unstable, the ''diffusivity'' of this term is negative. In (3.12b), all terms except the relaxation toward the radiative–convective equilibrium conspire to homogenize the vertically averaged potential temperature laterally.

The nonlinear terms in (3.12) all become singular when $yc^{-2}(\mathcal{M}^2)_y = \pi^4E^2$: in appendix B it is shown that this value coincides with the threshold for symmetric instability in the original set of equations (2.13). Moreover, the diffusivity in the quasi-linear term of the temperature equation [the term $\lambda F\alpha_2 N^2\Theta_y$ on the right-hand side of (3.12b)] becomes negative, even for positive prescribed stratification N^2. When the threshold of symmetric instability is passed, the validity of the evolution equations is lost: at the threshold of the instability, terms that were neglected become as large as those retained. The singularity signals a failure of our expansion. The regime where symmetric instability plays a role is certainly a very interesting one; however it will not be examined in this work.

The essential point emerging from (3.11) is that, in steady state, there is competition between advection, which tends to homogenize angular momentum, and surface drag, which injects horizontal gradients at the surface. Similarly, advection by the meridional cell homogenizes potential temperature laterally against the gradients imposed by the radiative equilibrium.

Both the nonlinear and the viscous terms in (3.11a) are in flux form and vanish when integrated over the domain. Thus, we have the kinematic condition

$$\int_{-1}^{1}\mathcal{M}_{t_1}\, dy = \gamma_2\int_{-1}^{1}(c^2 - \mathcal{M})\, dy, \tag{3.13}$$

which implies that, to first order, the horizontally averaged surface angular momentum spins down to the planetary value on a timescale inversely proportional to the surface drag. This implies that the net relative rotation rate of the atmosphere, ω_r, is $O(R)$ and is given by

$$\omega_r \equiv \int_0^1 dz\int_{-1}^{1} c^{-1}u\, dy = R\int_0^1 dz\int_{-1}^{1} dy c^{-2}M_1 + O(R^2). \tag{3.14}$$

Using the expressions for M_1 and ψ_0 in (3.7a,b) the net relative rotation rate is given by

$$\omega_r = R\int_{-1}^{1} c^{-2}\mathcal{M}_y\Theta_y\, dy\int_0^1 (1 - z)\phi(y, z)\, dz. \tag{3.15}$$

As long as the circulation is thermally and ''angular momentum'' direct, M_1 is positive everywhere in the domain and the net relative rotation of the atmosphere, ω_r, is eastward.

A kinematic constraint analogous to (3.13) exists for the vertically averaged potential temperature. Thus, integrating (3.11b) over the domain gives

$$\int_{-1}^{1}\Theta_{t_1}\, dy = \alpha_2\int_{-1}^{1}(\Theta_E - \Theta)\, dy. \tag{3.16}$$

Equation (3.16) simply states that advective and diffusive processes cannot change the volume-averaged potential temperature from that imposed by the radiative–convective equilibrium (the ''equal area'' rule).

4. Solutions with imposed stratification: $N^2 \neq 0$

Although (3.11) is considerably simpler than the two-dimensional system (2.13), its solutions depend on five parameters. (The original system has six parameters; our expansion has eliminated the Rossby number R.) Thus it is not possible to give a full description of the solution as a function of all parameters. We will therefore focus our attention on the range of parameters considered most relevant for the terrestrial circulation, that is, μ_2, $E \ll 1$ and α_2, $\gamma_2 \gg 1$, and $N^2 \lesssim 1$. The expansion culminating in (3.11) was derived under the assumption that all the parameters appearing in the final evolution equations are of order one. However, it is still possible to consider limiting cases and then check the consistency of the approximations a posteriori.

As a specific example we use the same form for the radiative–convective equilibrium temperature given by HH, that is, $\Theta_E = 4/3 - y^2$, and consider a set of parameter values examined in that reference, except that we have a nonzero horizontal diffusivity, $\nu_H \neq 0$:

$$\begin{aligned} \Omega &= 2\pi/(8.64 \times 10^4 \text{ s}) & \Delta_H &= 1/3 \\ a &= 6.4 \times 10^6 \text{ m} & \Delta_V &= 1/8 \\ g &= 9.8 \text{ m s}^{-2} & C &= 0.005 \text{ m s}^{-1} \\ H &= 8 \times 10^3 \text{ m} & \tau &= 20 \text{ days} \\ \nu_V &= 5 \text{ m}^2 \text{ s}^{-1} & \nu_H &= 1.86 \text{ m}^2 \text{ s}^{-1}. \end{aligned} \tag{4.1}$$

This choice is in the middle of the parameter range examined by HH (where $25 > \nu_V > 0.5$ m^2 s^{-1}, with all the other parameters fixed). The value of the lateral friction was dictated by computational reasons: it was the smallest that we could use without requiring an excessive amount of resolution. The choice in (4.1) leads to the following set of nondimensional values:

$$\begin{aligned} R &= 0.121 & \gamma_2 &= 550 \\ E &= 1.07 \times 10^{-3} & N^2 &= 0.045375 \\ \alpha_2 &= 509 & \mu_2 &= 4 \times 10^{-5}. \end{aligned} \tag{4.2}$$

Figure 1 shows $\mathcal{M}$, u, and Θ obtained by solving the steady version of (3.11) numerically.[1] Despite the large nondimensional relaxation constant, α_2, the vertically averaged potential temperature Θ is much more homogeneous than the radiative–convective equilibrium Θ_E in a region close to the equator that contains the bulk of ''the Hadley circulation.'' In the same region, however, there is no appreciable departure of the surface angular momentum $\mathcal{M}$ from the planetary value, c^2, so

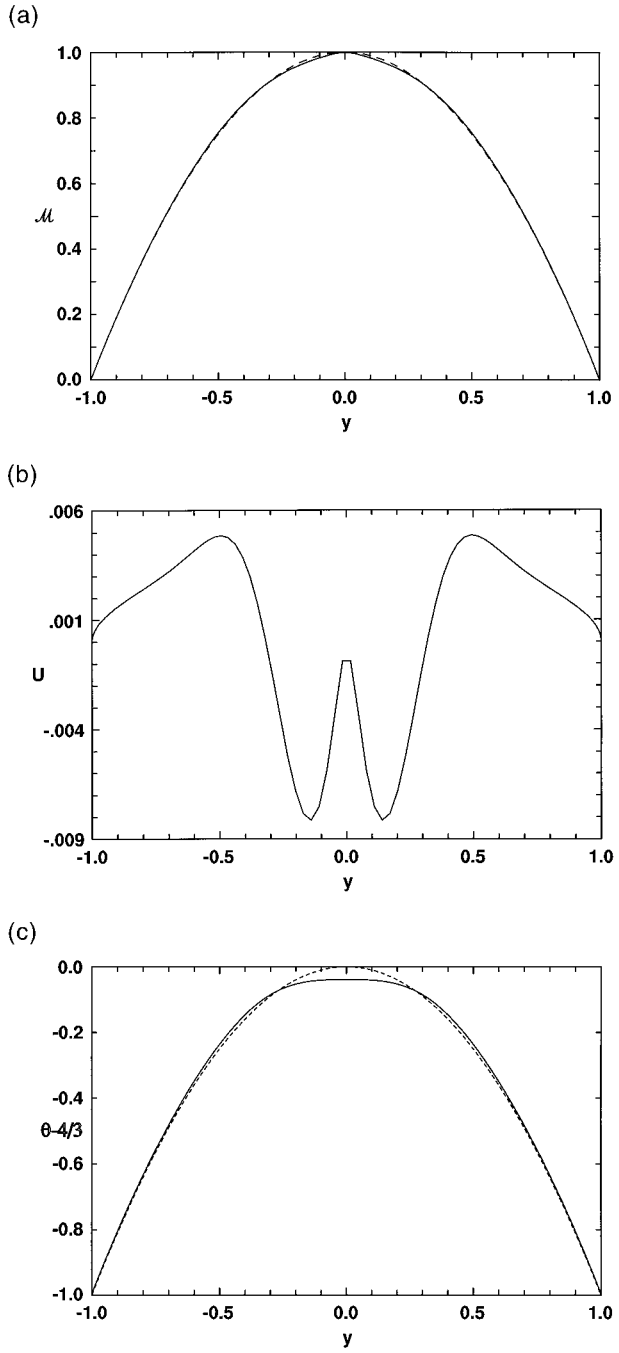

FIG. 1. Numerical solutions of (3.11) for the choice of parameter values given in (4.2) with $\Theta_E = 4/3 - y^2$. (a) The surface angular momentum $\mathcal{M}$ as a function of $y = \sin(\text{latitude})$ (solid line) compared to its planetary value, $1 - y^2$ (dashed line). For this large value of the nondimensional surface drag, $\gamma_2 = 550$, there is very little surface flow. Dimensional values for the surface angular momentum are obtained multiplying $\mathcal{M}$ by $\Omega a^2 = 2.979 \times 10^9$ m^2 s^{-1}. (b) The surface zonal wind U as a function of y. Dimensional values are obtained multiplying by $\Omega a = 465.4$ m s^{-1}. In this stretched coordinate system the area under the curve should vanish. (c) The vertically averaged potential temperature Θ (solid line) and radiative–convective equilibrium temperature Θ_E (dashed line) as a function of y: they differ in a region of order $\sqrt{N} = 0.21$, where Θ is homogenized. Dimensional values are obtained multiplying by $\Delta_H \theta_0 = 100$ K. The area between the solid and dashed curves should integrate to zero. Notice that it does so in a region that occupies the whole domain.

[1] To solve (3.11) numerically, $\mathcal{M}$ and Θ are expanded in Legendre polynomials (typically 200) and steady-state solutions are found using Newton–Keller's method. The analytic evaluation of the integrals involving ϕ in (3.11) were performed with the aid of the symbolic manipulation software MAPLE.

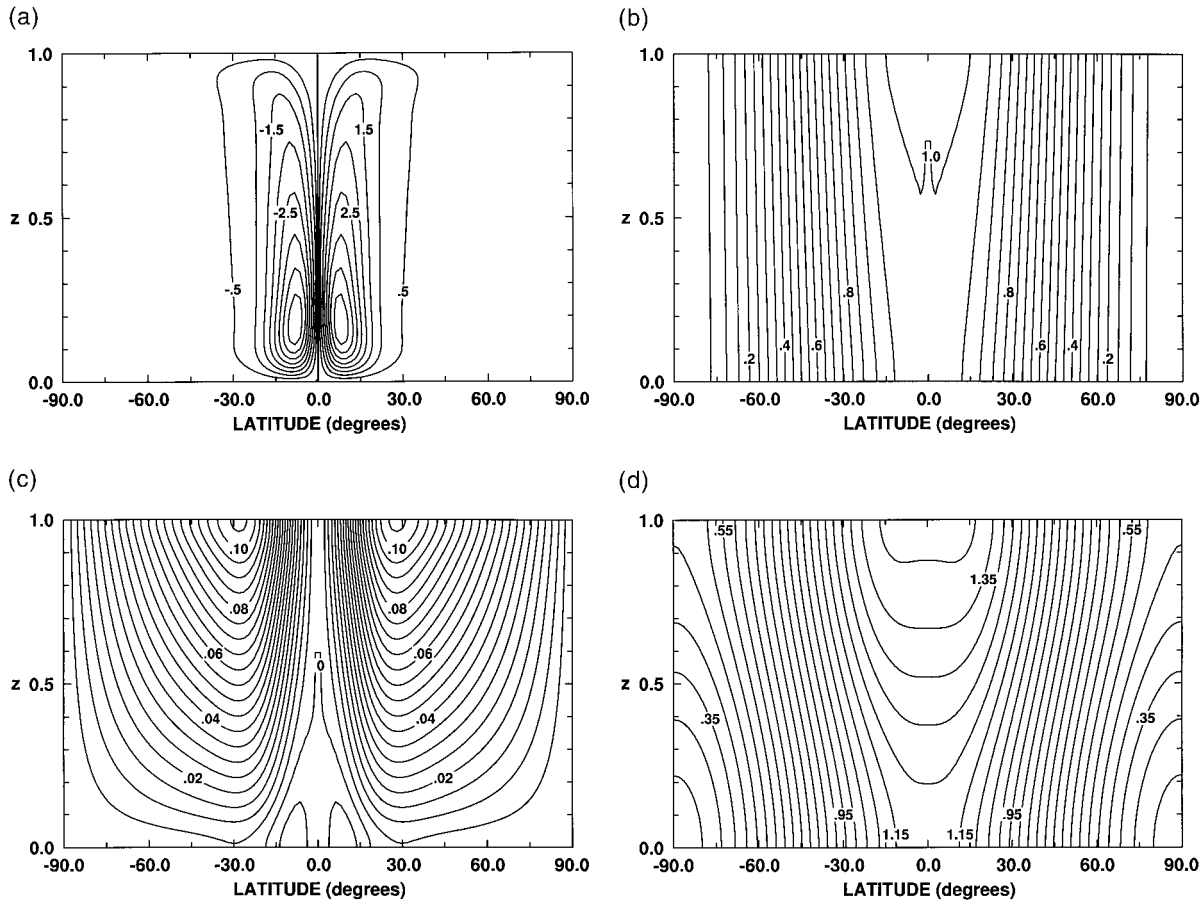

FIG. 2. Streamfunction, angular momentum, zonal wind, and potential temperature as a function of latitude and height corresponding to the numerical solution shown in Fig. 1. (a) The meridional streamfunction, $\psi_0 + R\psi_1$, obtained using (3.7), (A.3), and the solution to (C.4), for the calculations shown in Fig. 1. Dimensional values are obtained multiplying by $\nu_V R\epsilon^{-1} = 484$ m^2 s^{-1}. (b) The angular momentum, $\mathcal{M} + RM_1$. The baroclinic term, RM_1, reduces the lateral gradient of the angular momentum compared to its planetary value in a region that increases with height. For the Rossby number used here, $R = 0.121$, there is a small region of closed M contours signaling a failure of the asymptotic expansion. (c) The zonal velocity field, $U + Ru_1$. Dimensional values are obtained multiplying by $\Omega a = 465.4$ m s^{-1}. (d) The potential temperature field, $\Theta + R\theta_1$: as for the angular momentum the region of latitudinally homogenized potential temperature increases with height.

the angular momentum balance does not play a major role in the extent of the Hadley circulation for this parameter range [a result also found in the moist calculations of Satoh (1994)]. In Fig. 2 the first two terms in the expansion of the streamfunction, angular momentum, zonal velocity, and potential temperature fields are contoured in the meridional–vertical plane: for the last three fields the vertical structure appears at first order in the $O(R)$ correction and it is given in (3.7a,c). The calculation of ψ_1 in terms $\mathcal{M}$ and Θ is somewhat more laborious and can be found in appendix C. The agreement with the numerical results presented in HH (cf. the bottom panel in Fig. 4a of HH) is good: the structure of the streamfunction and of the zonal wind is well captured, and the maximum values of the meridional transport, the top and the bottom zonal winds in Fig. 2, are within 10% of the solution presented by HH (cf. the bottom panel in Fig. 4a of HH). However, there is a small region where closed angular momentum contours are found (see Fig. 2b), violating Hide's theorem.

The region of closed angular momentum contours coincides with the location of the breakdown of the approximation. Specifically in the upper equatorial region, for the choice of parameters in (4.2), the assumption that (M_0, T_0, ψ_0) is much greater than $R(M_1, T_1, \psi_1)$ is violated. In the following we will explain the parametric restrictions necessary to avoid this breakdown.

Steady solutions of (3.12) for $\alpha_2 N^2 \gg 1$, $\gamma_2 \gg 1$, $E \ll 1$, $\mu_2 \ll 1$, and $N^2 \ll 1$

With the hindsight afforded by the numerical solutions, it is not difficult to obtain approximate analytical solutions of (3.12). The first thing to notice is that for large γ_2 the surface angular momentum $\mathcal{M}$ is approximately clamped to the planetary value in the whole domain. Thus, the solution of (3.12a) is just

$$\mathcal{M} = 1 - y^2 + O(\gamma_2^{-1}). \tag{4.3}$$

This result implies that the surface zonal velocity is $O(\gamma_2^{-1}) \ll 1$. The reader might question the validity of (3.11) in this limit of large surface drag. We examine this issue in section 7 by returning to the full equations in (2.13) and making the expansion in $R \ll 1$, but with $\gamma = O(1)$, rather than $\gamma = O(R^2)$ as in (3.1). Based on this alternative expansion we conclude that (3.11) is valid even when $\gamma_2 \gg 1$. Thus, encouraged by the results of section 7, we continue with the solution of (4.3) in the limit $\gamma_2 \gg 1$. All the interesting information about the structure of the surface zonal wind is in the $O(\gamma_2^{-1})$ term of the expansion (4.3). In order to obtain this term we must first calculate the vertically averaged potential temperature Θ.

The strategy is to take advantage of the smallness of E, of α_2^{-1}, and of N^2 to simplify (3.12b) in nested equatorial regions of decreasing size and use matched asymptotics to construct a uniformly valid solution.

Because α_2 is very large there is an ''outer'' region, away from the equator, where Θ is clamped to the radiative–convective equilibrium Θ_E. As the equator is approached, there is a region within which Θ departs from Θ_E. In the limit of large α_2 and $N^2\alpha_2$, the term proportional to Θ_y^3 can be neglected in (3.12b), everywhere in the domain. Using the leading order term for $\mathcal{M}$ in (4.3), (3.12b) becomes (after division by α_2)

$$0 = 4/3 - y^2 - \Theta + N^2\left[\frac{8(1-y^2)\Theta_y}{\pi^4(\pi^4E^2 + 4y^2)}\right]_y + O(\alpha_2^{-1}, \gamma_2^{-1}, \mu_2). \tag{4.4}$$

For small N^2, the departures of Θ from the imposed equilibrium are small and confined to a small equatorial region of size $\delta \equiv \sqrt{N}$, making the analysis of (4.4) very simple.

Within the region of size δ it is useful to rescale $y = \delta\xi$. As long as $\xi \gg (E/\delta)$, we can neglect the term proportional to E so that (4.4) reduces to

$$0 = 4/3 - \delta^2\xi^2 - \Theta + \left(\frac{2\Theta_\xi}{\pi^4\xi^2}\right)_\xi + O(\delta^4). \tag{4.5}$$

In the context of the approximation $\delta \ll 1$ and $E \ll \delta$, the boundary conditions that ensure matching with the outer radiative–convective solution are

$$\Theta - 4/3 \to -\delta^2\xi^2 \quad \text{as } |\xi| \to \infty, \qquad \Theta_\xi(0) \quad \text{finite.} \tag{4.6a,b}$$

Although (4.5) can be solved exactly in terms of modified Bessel functions, it is more useful to look at the behavior of Θ for small ξ. There is a series solution of the form

$$\Theta - 4/3 = b(1 + \pi^4\xi^4/8 + \pi^8\xi^8/640 + \cdots) + \delta^2\pi^4\xi^6/60 + O(\xi^{10}), \tag{4.7}$$

where b is an unknown constant that is determined by requiring that the solution in (4.7) matches the outer solution in the limit $\xi \to \infty$ as required by (4.6a). A trick can be used to make this match: multiply (4.5) by a solution of the associated homogeneous problem, $h(\xi)$, and integrate over ξ from 0 to ∞. The homogeneous version of (4.5) has a solution that is regular at both $\xi = 0$ and $\xi = \infty$:

$$h(\xi) = \xi^{3/2}K_{3/4}(\sqrt{2}\pi^2\xi^2/4). \tag{4.8}$$

Multiplying (4.5) by $h(\xi)$ and integrating by parts then leads to

$$\delta^2\int_0^\infty \xi^2 h(\xi)\, d\xi = 2\pi^{-4}(\Theta(0) - 4/3)\lim_{\xi\to 0}\xi^{-2}h_\xi, \tag{4.9}$$

which gives

$$b = -2\delta^2\pi^{-5/2}\Gamma(3/4)^2 = -0.17168\delta^2. \tag{4.10}$$

This prediction agrees well with the numerical solution shown in Fig. 1.

To complete the analysis it is necessary to find the solution of (4.4) in the equatorial Ekman layer, that is, when $y = O(E)$. To this end, it is useful to introduce the boundary layer variable $\hat{y} \equiv y/(\pi^2E)$ and solve the rescaled form of (4.4),

$$8N^2\pi^{-12}\left[\frac{(1-\pi^4E^2\hat{y}^2)\Theta_{\hat{y}}}{1+4\hat{y}^2}\right]_{\hat{y}} = E^4(\Theta - 4/3 + \pi^4E^2\hat{y}^2). \tag{4.11}$$

The first terms in an expansion in powers of E^2 are

$$\Theta - 4/3 = b\left[1 + \frac{E^4\pi^{12}}{8N^2}\left(\frac{\hat{y}^2}{2} + \hat{y}^4\right)\right] + O(E^6). \tag{4.12}$$

Notice that the leading order term is the constant b, determined through matching with the solution (4.7) as $\xi \to 0$. In terms of the unscaled variable, y, the uniformly valid approximation to Θ, valid for small latitudes, is

$$\Theta - 4/3 \approx b[1 + \pi^4(E^2\pi^4y^2/2 + y^4)/(8N^2)]. \tag{4.13}$$

Figure 3 compares the approximation for Θ given in (4.13) (dotted line) with the values obtained for Θ by solving (3.12) numerically (solid line). There is excellent agreement in the region $y = O(\delta)$. Aside from the subdominant term of $O(E^2)$, the approximation (4.13) shows that the local behavior of the vertically averaged potential temperature gradient Θ_y near the equator is proportional to y^3 and not to y as imposed by the radiative–convective equilibrium (shown in Fig. 3 as a dashed line); that is, the thermal gradient is substantially weakened in the Hadley cell region.

We are now in a position to calculate the $O(\gamma_2^{-1})$ correction to the surface angular momentum and the $O(R)$ baroclinic correction to the total angular momentum. Using (3.7a,b), (4.13), and the first term of the series expansion (A.4) we find that near the equator

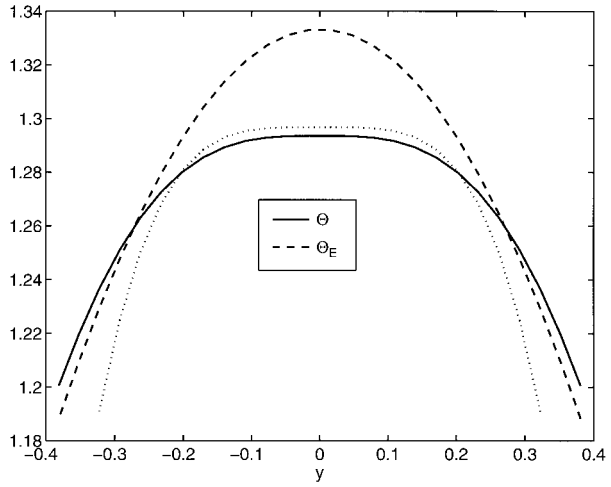

FIG. 3. The structure of the vertically averaged potential temperature near the equator for the parameter values used in Figs. 1 and 2. The solid line shows the solution for Θ obtained by solving (3.12) numerically. The approximation (4.13) is shown as a dotted line, and the dashed line is the radiative–convective equilibrium temperature, $\Theta_E = 4/3 - y^2$.

$$\mathcal{M} + RM_1 \approx 1 - y^2\left[1 + \frac{3\Gamma(3/4)^4\pi}{N^2\gamma_2} - \frac{2R\Gamma(3/4)^2}{\sqrt{\pi}N}(1 - \cos\pi z)\right]. \tag{4.14}$$

In the asymptotic limit $\gamma_2 \to \infty$, the baroclinic term in (4.14) (i.e., the third term in the square bracket) is much larger than the departures of $\mathcal{M}$ from the planetary value (the second term inside the square bracket). Notice that the baroclinic term tends to weaken the latitudinal gradient of the angular momentum in a region that expands with height. Thus, the angular momentum emerges from the upper branch of the Hadley cell with a gradient that is reduced from the planetary rest state. However, this quasi homogenization is achieved through viscous processes in this parameter range, as all the streamlines go through a bottom viscous boundary layer, precluding the applicability of Prandtl–Batchelor arguments.

The expression for M in (4.14) also allows one to determine the constraints on the Rossby number R in order for the perturbation expansion (3.3) to be uniformly valid. The region where the breakdown first occurs is at the top of the equatorial region, and the requirement that

$$RM_1(y = O(E),\, z = 1) \ll \mathcal{M}(y = O(E),\, z = 1) \tag{4.15}$$

is satisfied if

$$-2Rb\pi^2/N^2 \ll 1. \tag{4.16}$$

Using $b = -0.172\delta^2$ and $\delta^2 = N$ we find

$$R \ll N\sqrt{\pi}/[4\Gamma(3/4)^2] \approx 0.295N. \tag{4.17}$$

For the values used in the numerical calculation shown in Figs. 1 and 2, the constraint (4.17) is not satisfied and the approximation $\mathcal{M} \ll RM_1$ breaks down in a small region. However, there is a range in the Rossby number–stratification parameter space where the constraint (4.17) is satisfied. For example, with the value of N^2 used here, (4.17) is satisfied for $R \leq 0.06$, that is, half the value used in HH. Moreover, (4.17) is much less restrictive than the constraint $R \ll 80E^2$ found by Fang and Tung (1994) in the purely linear case [originally proposed by Charney (1973)].

Because in the range of large surface drag the angular momentum is, to leading order, equal to the planetary value, the solution for the streamfunction ψ_0 is equivalent to Charney's as long as the temperature gradient used is appropriately modified from the prescribed radiative–convective equilibrium.

The essential point is that, when N^2 is small but $\alpha_2 N^2$ and γ_2 are large, Θ is significantly different from Θ_E in a region of thickness $\sqrt{N} = (R\Delta_V/\Delta_H)^{1/4}$. The effect of the Hadley circulation is to homogenize the horizontal temperature gradient compared to the radiative–convective equilibrium prescription, and to reduce the vertically averaged equatorial potential temperature by an amount proportional to $N = (R\Delta_V/\Delta_H)^{1/2}$. Notice that in this limit in which the relaxation time τ is short compared to the viscous time H^2/ν_V, the extent of the Hadley circulation is independent of both these timescales.

In dimensional units, the size of the Hadley circulation is then given by $(a^2gH\Delta_V/\Omega^2)^{1/4}$, which corresponds to the equatorial Rossby radius of deformation, a scaling also suggested in Schneider and Lindzen (1976) and Schneider (1977).

The equatorial homogenization of the vertically averaged potential temperature is achieved through the meridional advection of the *baroclinic component* of potential temperature, which acts as an effective *lateral* diffusion with a diffusivity proportional to the vertical stratification: this is the term $(\lambda F\alpha_2 N^2\Theta_y)_y$ in (3.12b). However, unlike the linear model analyzed by Schneider and Lindzen (1976), the vertical stratification is not clamped to the radiative–convective equilibrium but is determined through a diffusive balance. This is quite apparent in Fig. 4, where we compare the departures from the vertically averaged potential temperature prescribed by the radiative–convective equilibrium to the vertically varying potential temperature obtained in our expansion, evaluated at the equator, that is, $R\theta_1$ obtained from (3.7c). The two fields differ in two thick diffusive layers next to the two boundaries. Despite the apparently diffusive and viscous nature of the balances analyzed here the final amplitude and scale of the temperature field are independent of viscosity.

5. Solutions with no imposed stratification: $N^2 = 0$

A model of the symmetric circulation should consider the meridional motion that develops in response to the

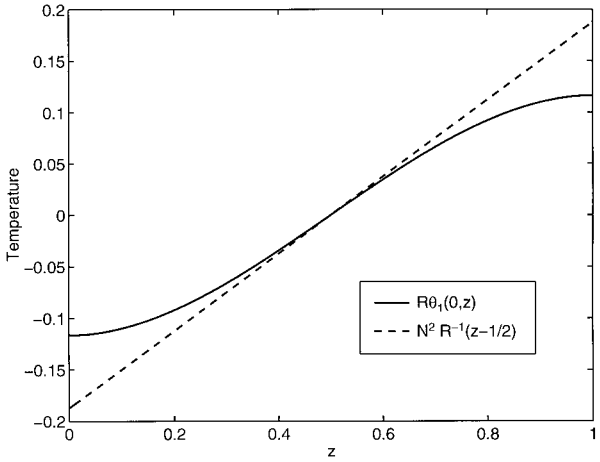

FIG. 4. The vertically varying part of potential temperature at the equator as a function of z as prescribed by the radiative–convective equilibrium, $N^2R^{-1}(z - 1/2)$, (dashed) and from the expansion in small Rossby number, $R\theta_1$ with θ_1 given by (3.7c) (solid).

distribution of temperature imposed by the radiative–convective equilibrium. The main role of nonhydrostatic convection is to erase the unstable stratification built by the radiative equilibrium alone: we thus expect that convective processes would leave the atmosphere in a state of neutral vertical stratification. However, because moisture is an essential element of tropical convection, potential temperature will follow a moist adiabatic profile, which corresponds to stably stratified potential temperature. In the context of a conceptual dry model, it is reasonable to analyze the consequences of ''dry convection'' and assume that the radiative–convective equilibrium leaves the atmosphere in a neutrally stratified state; that is, $N^2 = 0$. The solution in the previous section depended crucially on the assumption that $N^2 \neq 0$. In this section we examine the qualitative changes contingent upon taking $N^2 = 0$.

Figure 5 shows $\mathcal{M}$, U, and Θ resulting from a numerical solution of (3.11) for the same parameter values given in (4.1) and (4.2) except that now $N^2 = 0$. Despite the large value of the surface drag, there is now an equatorial region where the surface angular momentum (shown in Fig. 5a) departs from the planetary value and is homogenized. The vertically averaged potential temperature is homogenized in a region of similar extent (Fig. 5c). This leads to easterly surface winds that are maximum at the equator (Fig. 5b) and westerlies that are stronger than those obtained if $N^2 \neq 0$ (cf. Fig. 1b).

Inside the ''cavity'' of homogenized $\mathcal{M}$ and Θ there is a tight meridional circulation, as shown in Fig. 6a. Because the stratification produced by the meridional circulation is proportional to the square of the latitudinal temperature gradient [see the term $\Theta_y^2\phi$ in (3.7c)] the homogenized equatorial cavity is unstratified, as illustrated in Fig. 6d.

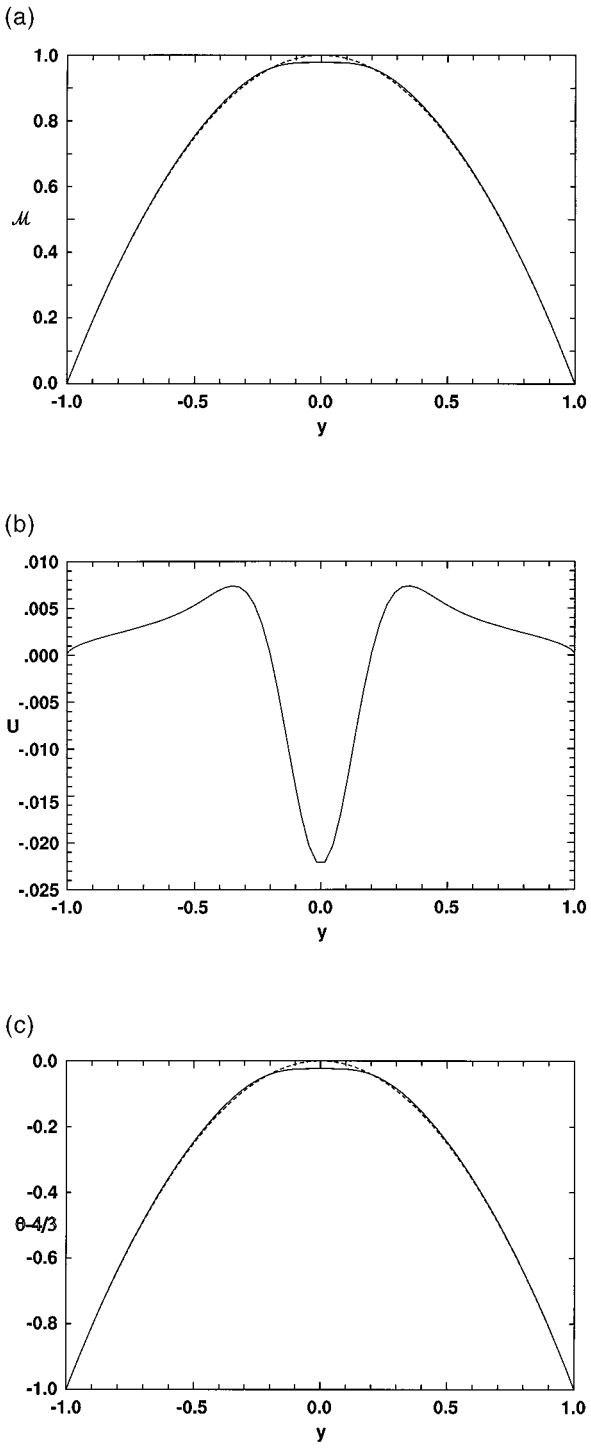

FIG. 5. Numerical results for the same parameter values used in Fig. 1 except that $N^2 = 0$. (a) The surface angular momentum, $\mathcal{M}$ as a function of y (solid line) compared to its planetary value, $1 - y^2$ (dashed line); $\mathcal{M}$ is homogenized in a region of size $\gamma_2^{-1/4}$ centered at the equator. (b) The surface zonal wind U, as a function of y, displays maximum easterlies at the equator. (c) The vertically averaged potential temperature $\Theta - 4/3$ (solid line) and radiative–convective equilibrium potential temperature, $\Theta_E - 4/3 = -y^2$ (dashed line) as a function of y. For this parameter range where $\alpha_2 \approx \gamma_2$ the region of homogenized Θ coincides with the region of homogenized $\mathcal{M}$.

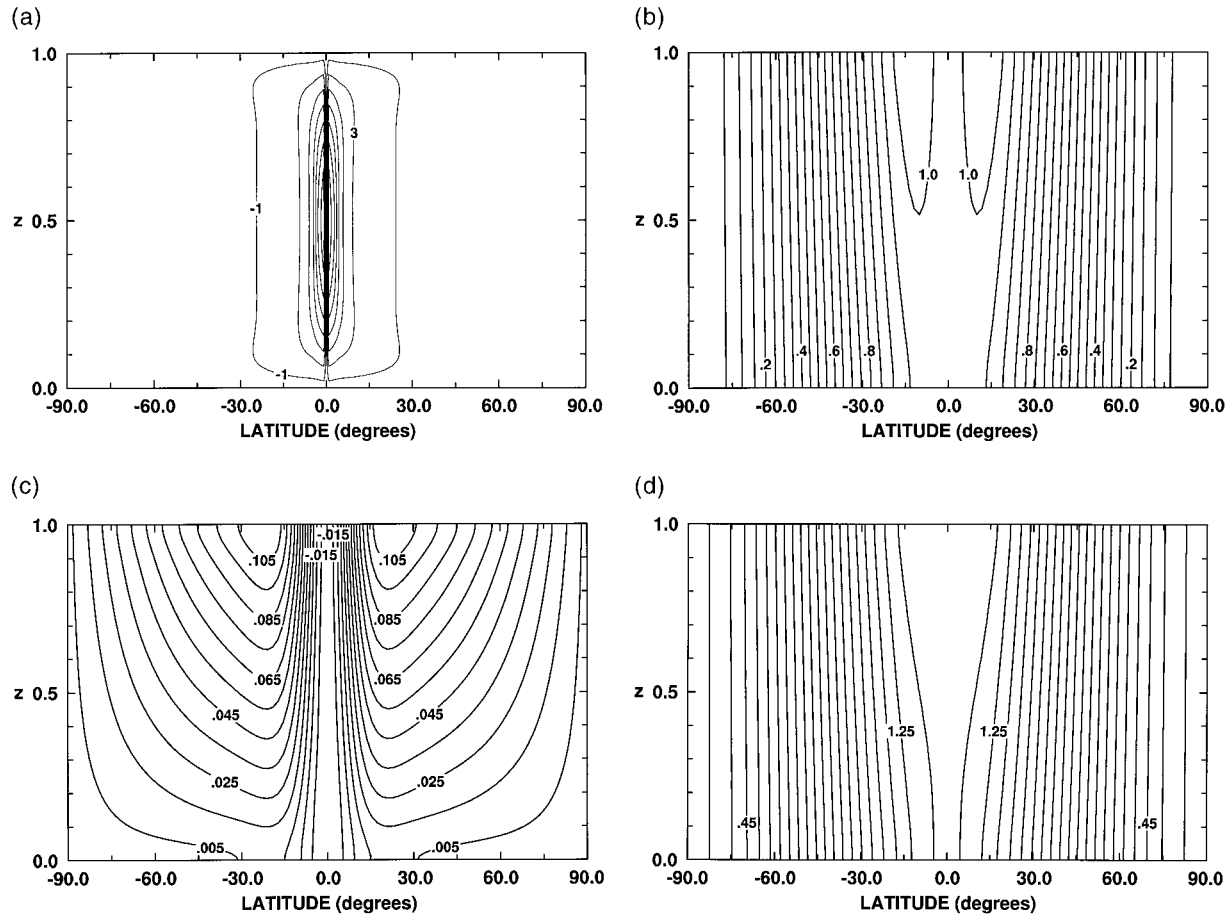

FIG. 6. Streamfunction, angular momentum, zonal wind, and potential temperature as a function of latitude and height corresponding to the numerical solution shown in Fig. 5. (a) The meridional streamfunction at the lowest order approximation ψ_0. The contour interval is 2.0. (b) The angular momentum, $\mathcal{M} + RM_1$, is homogenized within the Hadley cell. The baroclinic term, RM_1, exceeds the depth independent part $\mathcal{M}$ in a small region. (c) The zonal velocity field, $U + Ru_1$. The equatorial region is dominated by a barotropic core of easterlies. (d) The potential temperature field, $\Theta + R\theta_1$: without externally imposed stratification the equatorial region is vertically and horizontally homogeneous, and the dynamically driven stratification is maximum in the tropical band where the horizontal temperature gradients are the largest.

Steady solutions of (3.12) for $\alpha_2 = \gamma_2 \gg 1$, $E \ll 1$, $\mu_2 \ll 1$, and $N^2 = 0$

In the following approximate solutions in this range are presented. As in the analysis of section 4, we first consider the outer region of the meridional circulation, corresponding to its descending branch (cf. Fig. 6a). In this region, the terms proportional to E and μ_2 can be neglected and we have the approximate balance

$$0 \approx \gamma_2(c^2 - \mathcal{M}) + \left(\frac{8c^6\Theta_y^2}{4\pi^2 y^2 \mathcal{M}^2 \mathcal{M}_y}\right)_y$$

$$0 \approx \alpha_2(\Theta_E - \Theta) + \left(\frac{8c^6\Theta_y^3}{4\pi^2 y^2 \mathcal{M}^2 \mathcal{M}_y^2}\right)_y. \qquad (5.1)$$

In the special case when $\alpha_2 = \gamma_2$, this formidable-looking system can be solved, at least when $\Theta_E = 4/3 - y^2$, by noticing that the solution must satisfy $\mathcal{M} - 1 = \Theta - 4/3$. Numerical exploration shows that the qualitative character of the solution for $\alpha_2 = \gamma_2$ is unchanged when $\alpha_2 \approx \gamma_2$. Then $\mathcal{M}$ (or Θ) satisfies

$$0 \approx \gamma_2(c^2 - \mathcal{M}) + \left(\frac{2c^6\mathcal{M}_y}{\pi^2 y^2 \mathcal{M}^2}\right)_y. \qquad (5.2)$$

In the large γ_2 limit, we anticipate that the departures of $\mathcal{M}$ from the local planetary value will be of small amplitude and confined to a small equatorial region and seek a solution of (5.2) in the form $\mathcal{M} = 1 + \delta^2 m(\xi)$, where $\delta \equiv (\gamma_2)^{-1/4}$ is the characteristic size of the Hadley cell and $\xi \equiv y/\delta$. Then in the limit of small δ, (5.2) becomes

$$0 = -(\xi^2 + m) + \left(\frac{2m_\xi}{\pi^2 \xi^2}\right)_\xi + O(\delta^2), \qquad (5.3)$$

which has the same form as (4.5). Using the method outlined in section 4 we find that the local behavior of m is

$$m = a_0(1 + \pi^2\xi^4/8) + O(\delta^2, \xi^6),$$
$$a_0 = -2\pi^{-3/2}\Gamma(3/4)^2. \quad (5.4)$$

The local solution (5.4) shows that the meridional circulation reduces the gradient of the angular momentum $\mathcal{M}$. The local dependence of $\mathcal{M}$ within the ascending branch of the meridional circulation is given by a constant, which is less than unity, implying surface easterlies at the equator. The variation with latitude of the angular momentum is proportional to the *fourth* power of $y = \delta\xi$ rather than the variation imposed by solid-body rotation y^2. Because of the kinematic constraint (3.13), the gradients induced by the solid-body rotation are expelled outside the region of meridional circulation, giving rise to surface westerlies (cf. Fig. 5b).

Because of viscous effects, the close neighborhood of the equator needs a careful treatment. In the range $1 \gg E \gg \mu_2$, the assumption that E^2 is much less than $y(\mathcal{M}^2)_y$ in (3.12), with $\mathcal{M}$ given by (5.4), breaks down in an equatorial boundary layer of size $\sqrt{E\delta}$. Here we are assuming that $\delta \gg E$ so that the viscous sublayer is smaller than the characteristic size of the Hadley cell, δ. In this viscous region we adopt the rescaling

$$\eta \equiv y/\sqrt{E\delta},$$
$$\mathcal{M} - 1 = a_0\delta^2 + E^2 m_1(\eta). \quad (5.5)$$

The rescaled form of (3.12) then reads

$$a_0 + E\delta^{-1}\eta^2 + E^2\delta^{-2}m_1 = \left[\frac{8m_{1\eta}^3}{\pi^2(\pi^4 - 2\eta m_{1\eta}(1 + a_0\delta^2 + E^2 m_1))^2}\right]_\eta, \quad (5.6)$$

so the dominant balance is

$$a_0\eta = \frac{8m_{1\eta}^3}{\pi^2(\pi^4 - 2\eta m_{1\eta})^2} + O(\delta^2, E\delta^{-1}). \quad (5.7)$$

It is now clear that close to the equator $m_1 \approx 3(\pi^{10}a_0\eta^4)^{1/3}/8$, and a singularity at the equator appears in the *second derivative* of the angular momentum and temperature. In terms of the nondimensional latitude y, this corresponds to

$$\mathcal{M} - 1 = a_0\gamma_2^{-1/2} + 3(\pi^{10}a_0)^{1/3}E^{4/3}\gamma_2^{1/6}y^{4/3}/8. \quad (5.8)$$

This weak singularity in the angular momentum and in the potential temperature is healed by the explicit lateral diffusion, proportional to μ_2, in a very small sublayer (poorly resolved in the numerical calculation shown in Figs. 4 and 5). Naturally, the nonanalytic behavior of the solution is cause of a failure of the ordering of the perturbation expansion: $R\psi_1$ becomes larger than ψ_0, $R^2\Theta_2$ becomes larger than $R\Theta_1$, and so forth as the equator is approached. This singularity in high derivatives (here the second derivative of the relevant dynamical fields) is reminiscent of the difficulties encountered in critical layers and signals the local importance of neglected processes, for example, lateral friction or time dependence. A detailed analysis of this equatorial "critical layer" would require examination of the full system (2.13) and it is beyond the scope of this presentation. We conjecture that, given the weakness of the singularity, the approximate behavior of the surface angular momentum and vertically averaged potential temperature given in (5.4) and (5.7) is essentially correct.

In summary, we find that if the radiative–convective equilibrium does not impose explicit stratification, the downgradient mixing due to the meridional circulation reduces the gradient of the surface angular momentum as well as the gradient of the vertically averaged potential temperature. Because of the "equal-area rule" for the surface angular momentum (3.13) the equatorial value of $\mathcal{M}$ is less than that of the rest state. This leads to surface easterlies at the equator, at least in the limited range of parameters explored, even for temperature distributions that are latitudinally symmetric. This result has a certain appeal because in previous work (Lindzen and Hou 1988) surface equatorial easterlies have been attributed to distributions of equilibrium temperatures that are centered off the equator. However, for latitudinally asymmetric temperature distributions, the model (2.13) is very prone to symmetric instabilities.[2]

Homogenization of $\mathcal{M}$ and Θ leads to homogenization of the whole θ and M fields: recall that the corrections to the vertically homogenous fields, $\mathcal{M}_1$ and θ_1 given in (3.7), are proportional to the *lateral* gradients of $\mathcal{M}$ and Θ. Therefore, in the region where $\mathcal{M}$ and Θ are homogeneous, no vertical gradients are generated.

The approximate analytic solutions show that the extent of the Hadley cell, defined as the region where the surface angular momentum and the vertically averaged potential temperature depart substantially from the rest states, is proportional to

$$\gamma_2^{-1/4} = (R^2\nu_V/CH)^{1/4},$$

and the maximum surface easterlies are proportional to $R\sqrt{\nu_V/CH}$.

Thus, at least in the limit examined in this section, the size of the Hadley cell depends on the bottom drag ν_V/CH.

6. Solutions with weak surface drag, $\gamma_2 = O(1)$

Gradient expulsion of angular momentum is most dramatic when unimpeded by surface drag. In the regime where γ_2 is not large, the region of homogenized angular momentum occupies a considerable portion of the spherical shell and the surface winds are strong. Figure 7 shows $\mathcal{M}$, U, and Θ obtained by solving the steady ver-

[2] Indeed, when we forced the steady version of (3.11) with asymmetric temperature distributions a la Lindzen and Hou (1988), the surface angular momentum at the equator satisfied the condition $y(\mathcal{M}^2)_y < \pi^4E^2$; that is, it was symmetrically unstable.

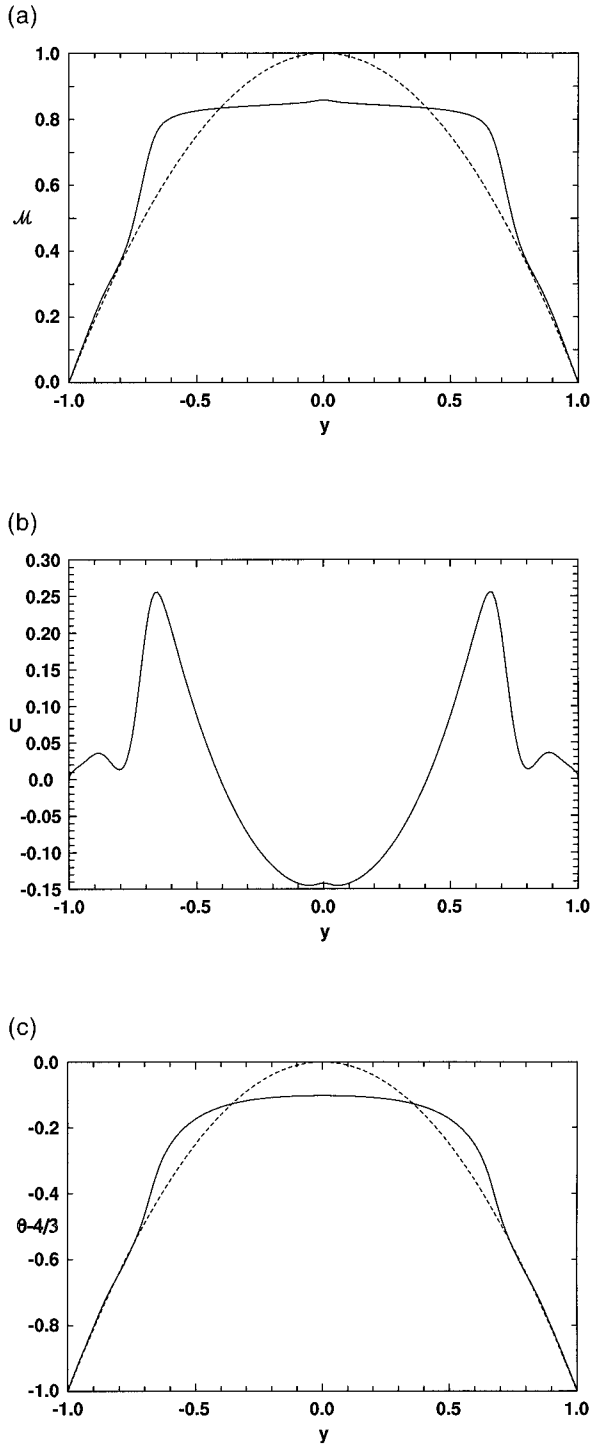

FIG. 7. Numerical results for the same parameter values used in Fig. 1 except that $\gamma_2 = 24$. (a) The surface angular momentum $\mathcal{M}$ as a function of y (solid line) compared to its planetary value, $1 - y^2$ (dashed line); $\mathcal{M}$ is homogenized in a region of order one. (b) The surface zonal wind U, as a function of y, displays maximum easterlies at the equator and large westerlies in midlatitudes. (c) The vertically averaged potential temperature $\Theta - 4/3$ (solid line) and radiative–convective equilibrium potential temperature, $\Theta_E - 4/3 = -y^2$ (dashed line) as a function of y. Despite the large value of α_2 the region of homogenized Θ is of $O(1)$.

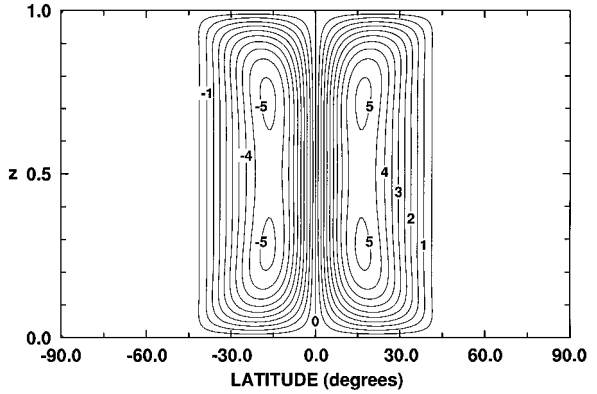

FIG. 8. Contours of the meridional streamfunction at the lowest order approximation, ψ_0, for the parameter values considered in section 6 and Fig. 7. A vigorous circulation is obtained in the region of homogenized $\mathcal{M}$ and Θ, and the gradients of both quantities are expelled at the outer edges of the cells.

sion of (3.11) numerically using the parameter values given in (4.2) except that

$$\gamma_2 = 24. \tag{6.1}$$

In this parameter range, angular momentum is the leading field: because the weak surface drag allows homogenization of $\mathcal{M}$, the potential temperature gradients are also expelled. Recall that when angular momentum is homogenized, ϕ, solution of (3.8) approaches the nonrotating limit, which implies a very vigorous meridional circulation. However, this strong meridional flow equilibrates to a lower value by mixing Θ despite the fast temperature relaxation time (here $\alpha_2 = 509$). The circulation that results from this balance, represented by the leading order streamfunction ψ_0 in Fig. 8, is indeed of $O(1)$ and not of $O(E^{-2})$ as in the nonrotating regime.

The range of parameters described in this section is not easily amenable to analytical exploration, but it appears to approach the ideal situation envisaged in HH: inside the meridional overturning cells angular momentum is conserved (here it is almost homogeneous), while outside it is given by the planetary value. This is best illustrated in Fig. 9a, where we show the vertical vorticity at the surface, $-\partial_y \mathcal{M}$: internal boundary layers connect the equatorial region of almost zero vorticity with the polar regions where $-\partial_y \mathcal{M} \approx 2y$, that is, the planetary gradient. The region of zero vertical vorticity coincides with the meridional circulation (cf. Fig. 8). The potential temperature exhibits a behavior analogous to the angular momentum: inside the meridional cell potential temperature gradients are very small, while outside Θ hugs the radiative–convective equilibrium Θ_E. The contrast between the two behaviors is most apparent if the potential temperature gradient, shown in Fig. 9b, is examined. Thick internal boundary layers connect the equatorial region characterized by weak gradients with the high latitudes where $\partial_y \Theta \approx \partial_y \Theta_E$.

However, while the emphasis in HH is on the *baro-*

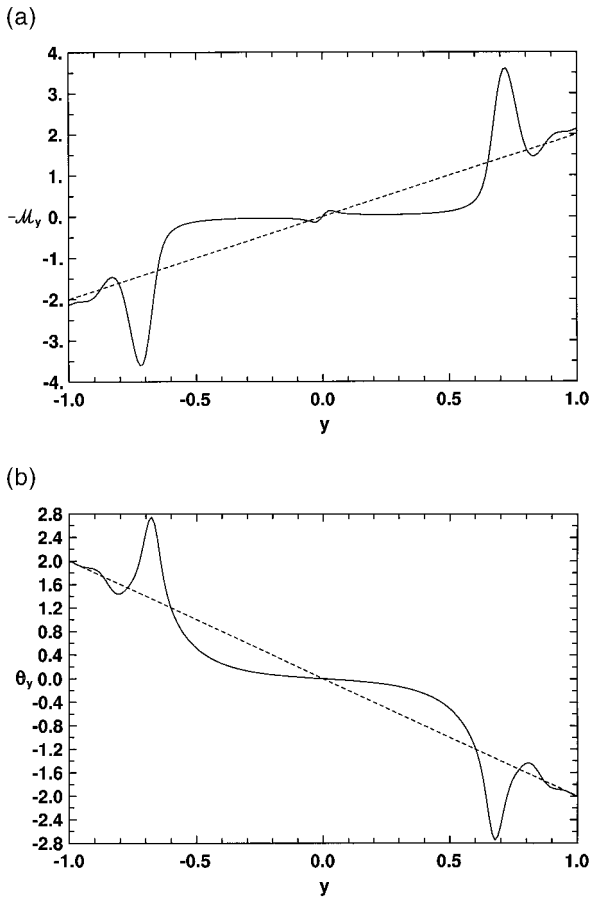

FIG. 9. (a) The vertical component of the surface vorticity, $-\partial_y \mathcal{M}$, as a function of latitude (solid line). Internal boundary layers located at the edge of the meridional cell (cf. Fig. 8) connect the regions of almost zero $-\partial_y \mathcal{M}$ with the polar regions where the surface vorticity approaches the planetary gradient, $2y$ (dashed line). (b) The latitudinal gradient of the vertically averaged potential temperature $\partial_y \Theta$ (solid line) and of the radiative–convective equilibrium $\partial_y \Theta_E$. Internal boundary layers connect a region of vanishing gradient with the region in radiative–convective equilibrium, where $\partial_y \Theta \approx \partial_y \Theta_E$.

clinic component of the angular momentum, here the small surface drag allows a large *barotropic*, depth-independent part of the angular momentum to dominate. Numerical calculations varying the parameter γ_2 in a range of $O(1)$, not presented here, show that the scale of the circulation is dictated by the value of the surface drag γ_2. Notice also that the surface wind at the equator is negative and large. In this sense, the regime shown in Figs. 7 and 8 is akin to the unstratified case, described above, even though stratification is present. As in the unstratified case, weak singularities in the high derivatives of $\mathcal{M}$ and Θ develop unless regularized by the explicit lateral diffusion term proportional to μ_2.

7. Asymptotic reduction in the limit of large surface drag

In the previous sections we have seen that the qualitative structure of the solutions depends crucially on the surface drag γ_2. It is important to understand how the asymptotic reduction changes if one makes alternative scaling assumptions about bottom drag. Recall that in (3.1) we wrote $\gamma = R^2\gamma_2$ and held γ_2 fixed as $R \to 0$. This ensured that the velocity at both $O(1)$ and $O(R)$ satisfied a free-slip condition on the ground. Now we will consider an alternative scaling in which γ is held fixed as $R \to 0$. In this case the velocities satisfy a mixed boundary condition at the ground at all orders. We will show that the evolution equations hold their validity even in this limit. To do this we quickly rederive the $O(R^2)$ balance and solvability condition assuming that $\gamma = O(1)$. In the limit of $R \ll 1$, and regardless of the size of γ, we still expand all fields in powers of R as in (3.3).

The terms of $O(R^0)$ in the system (2.13) are still given by (3.4); however, now the boundary condition at $z = 0$ is $M_{0z} = \gamma(M_0 - c^2)$. Thus, the solution to (3.4) is

$$M_0 = c^2, \qquad \theta_0 = \Theta(y, t_1). \tag{7.1}$$

Comparing (7.1) with (3.5) shows that the promotion of γ to $O(1)$ from $O(R^2)$ (as was the case in section 3) leads to the demotion of the angular momentum from its former prognostic prominence. Now M_0 is clamped to the planetary value c^2 and only the vertically averaged temperature remains as a ''master variable.''

The $O(R)$ balance is as in (3.6) and (3.7), that is,

$$\begin{aligned} M_{1z} &= -\psi_0(c^2)_y, \\ \psi_0 &= -\Theta_y \phi(z, y), \\ \Theta_{1z} &= \frac{1}{2}\alpha_2 N^2 z(1 - z) + \Theta_y^2 \phi(z, y). \end{aligned} \tag{7.2}$$

The boundary condition at $z = 0$, $M_{1z} = \gamma M_1$, together with (7.2a) implies that both M_1 and M_{1z} vanish at the bottom, since $\psi_0|_{z=0} = 0$. The vertical structure of the meridional streamfunction ϕ satisfies

$$E^2\phi_{zzzz} - 2y(c^2)_y\phi = c^2, \tag{7.3}$$

subject to the boundary conditions $\phi = \phi_{zz} = 0$ at $z = 1$, and $\phi = \phi_{zz} - \gamma\phi_z = 0$ at $z = 0$. It will be apparent shortly that the different bottom boundary condition for ϕ is the main point of departure between the evolution equations given in this section and those given in section 3. However, in the limit of small Ekman number E, the difference between the solution of (7.3) and the solution of (3.8) is confined to a thin bottom boundary layer of thickness $\sqrt{E}$.

In anticipation of the $O(R^2)$ balance, we compare in Fig. 10 the vertical average of ϕ^2 for $\gamma = 0$, that is, the assumption made in section 3, and for $\gamma = 10$. When the Ekman number is small, which is the limit of interest here, the two integrals differ by a small amount.

In parallel with the procedure detailed in section 3c, a solvability condition emerges when the $O(R^2)$ angular momentum and potential temperature equations are vertically integrated, namely,

$$0 = -\gamma M_2|_{z=0} + \left[c_y^2\Theta_y^2 \int_0^1 \phi^2\, dz\right]_y,$$

$$\Theta_{t_1} = \alpha_2(\Theta_E - \Theta) + \left[\Theta_y^3 \int_0^1 \phi^2\, dz + \frac{1}{2}\alpha_2 N^2\Theta_y \int_0^1 z(1-z)\phi\, dz + \mu_2 c^2\Theta_y\right]_y. \quad (7.4)$$

The evolution equation for the vertically averaged potential temperature Θ is formally the same as that found in section 3c, except for the already noted difference in ϕ and, most importantly, for the fact that Θ is determined independently of M_2. Indeed, (7.3) shows that ϕ is independent of M_2 because the surface angular momentum is, to a first approximation, clamped to the planetary value. In this sense, the potential temperature is a master variable: it is determined independently of the unknown contribution to the surface angular momentum M_2.

On the other hand, the solvability condition (7.4a) determines the surface value of M_2 in terms of Θ. In this sense the angular momentum is a ''slave variable'' (as is ψ): its distribution in space and time is dictated by Θ.

Despite this important difference, (7.4a) is actually equivalent to taking the limit $\gamma_2 \gg 1$ in the ''master equation'' (3.11a), as it is appropriate in the range $\gamma = O(1)$ and $R \ll 1$. In that limit, as shown in section 4, (3.11a) can be solved perturbatively; that is,

$$\mathcal{M} = c^2 + \gamma_2^{-1} m_1 + O(\gamma_2^{-2}). \quad (7.5)$$

Sustituting the expansion (7.5) in (3.11a) and collecting the terms of $O(1)$ we find that m_1 satisfies

$$0 = -m_1 + \left[c_y^2\Theta_y^2 \int_0^1 \phi^2\, dz\right]_y + O(\gamma_2^{-2}). \quad (7.6)$$

Using (7.5) and recalling that $\gamma_2 \equiv R^{-2}\gamma$ and that $\mathcal{M}$ is defined to be the surface angular momentum, $M(y, 0, t_1)$, (7.6) can be rewritten as

$$0 = \gamma R^{-2}(c^2 - M(y, 0, t_1)) + \left[c_y^2\Theta_y^2 \int_0^1 \phi^2\, dz\right]_y + O(\gamma_2^{-2}). \quad (7.7)$$

Now it is clear that (7.4a) is equivalent to (7.7) up to $O(R^2)$, because

$$R^{-2}(M(y, 0, t_1) - c^2) = M_2(y, 0, t_1).$$

In summary, we find that the choice $\gamma = O(R^2)$ in the small Rossby number limit leads to an evolution equation for the surface angular momentum, that is, (3.11a), which is more general than that obtained for the choice $\gamma = O(1)$. Specifically, (7.4a) is a limiting case of (3.11a) when $\gamma_2 \gg 1$.

8. Summary and conclusions

We have tried to understand the contradictory role of friction in the axially symmetric circulation on a rapidly rotating planet, driven by meridional thermal gradients. Recognizing that meridional motions rely on friction leads us to postulate that the strength of the meridional overturn is directly proportional to the explicit viscosity ν_V, as is the case for Charney's linear model. Despite this conjecture, it is still possible to consider the limit of small dissipation by considering the Ekman number to be small. Our formulation is consistent with the notion of weakly dissipated and weakly forced flows where the streamlines are aligned with the quasi-conserved quantities, here the angular momentum and the potential temperature, everywhere except in thin boundary layers.

The compromise between a weak circulation and a quasi-inviscid, fully nonlinear balance is possible in the limit of small Rossby number R as long as a distinguished limit relating the nondimensional parameters of the problem to R is considered. This contrived range of parameters is not always within the reach of atmospheric values, but it allows the explicit calculation of the advective fluxes in terms of two fundamental variables: the surface angular momentum and the vertically averaged potential temperature. One result is that the meridional circulation induces a stably stratified vertical temperature gradient, proportional to the *square* of the horizontal temperature gradient, by tilting the latitudinal gradients generated by the differential solar heating. Thus, even if the radiative–convective equilibrium has no vertical stratification, the large-scale dynamics can supply one. The same tilting mechanism turns horizontal gradients of angular momentum, provided by the earth's rotation and by relative rotation, into vertical angular momentum gradients, that is, zonal wind shears. The constraint that this dynamically induced vertical shear is in cyclostrophic balance determines the meridional circulation in the interior.

The overturning of these dynamically generated vertical gradients in turn changes the *horizontal* gradients of potential temperature and angular momentum from the values prescribed by the solar heating and the planetary rotation respectively. Specifically, the meridional flow acts to diffuse laterally and downgradient angular momentum and potential temperature. This is a reassuring result: lateral homogenization of potential temperature near the equator is an observed feature, while

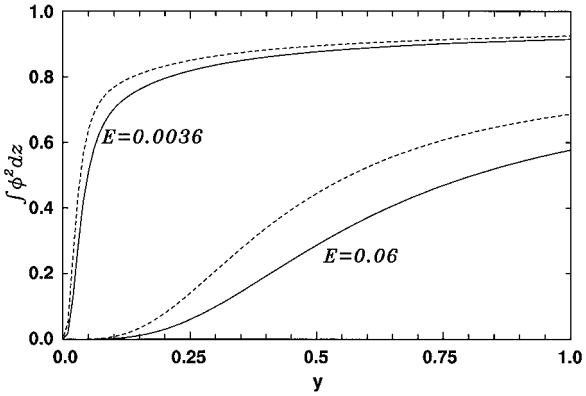

FIG. 10. The vertical average of ϕ^2, solution of (7.3) with boundary conditions $\phi = \phi_{zz} = 0$ at $z = 1$, and $\phi = \phi_{zz} - \gamma\phi_z = 0$ at $z = 0$, for different values of γ and the Ekman number E. The solid lines have $\gamma = 10$, that is, the no-slip bottom boundary condition is approached, and the dashed lines have $\gamma = 0$; this is the no-stress case considered in section 3. For small Ekman number the integrals differ by an amount of order $\sqrt{E}$.

angular momentum homogenization has often been advocated (e.g., Bretherton and Turner 1968) and has been also obtained in some numerical solutions (e.g., Satoh 1994).

While there is quantitative agreement of our solutions with some of the numerical computations presented in HH, the calculations in HH with very small viscosity differ from those found here. Specifically, the calculations published in HH show a qualitative change as $\nu_V \to 0$. In Fig. 11 we plot the ratio of the dimensional streamfunction maxima to the vertical viscosity as a function of ν_V for the sequence shown in HH (their Fig. 4). The analysis presented in section 4 predicts that ψ_0, marked by circles in Fig. 11, is approximately independent of ν_V. If the $O(R)$ correction is added to the streamfunction (diamonds) a weak dependence upon ν_V emerges, but the qualitative structure of the streamfunction is as shown in Fig. 2.

The numerical results of HH, marked by squares in Fig. 11, show that, for $\nu_V \geq 2.5$, the streamfunction maxima scale approximately linearly with ν_V, as predicted by our reduction. For $\nu_V < 2.5$, $\psi_{\max}/\nu_V$ rapidly increases as viscosity decreases. This sudden increase is accompanied by a qualitative change in the streamfunction structure: the position of the streamfunction maximum in HH moves from the bottom of the vertical domain to the top (cf. Fig. 4 in HH). We conjecture that, in this range of small viscosity, a symmetric mode, which is only very weakly damped, can be nonlinearly excited, leading the system through a bifurcation that is not captured by our reduction.

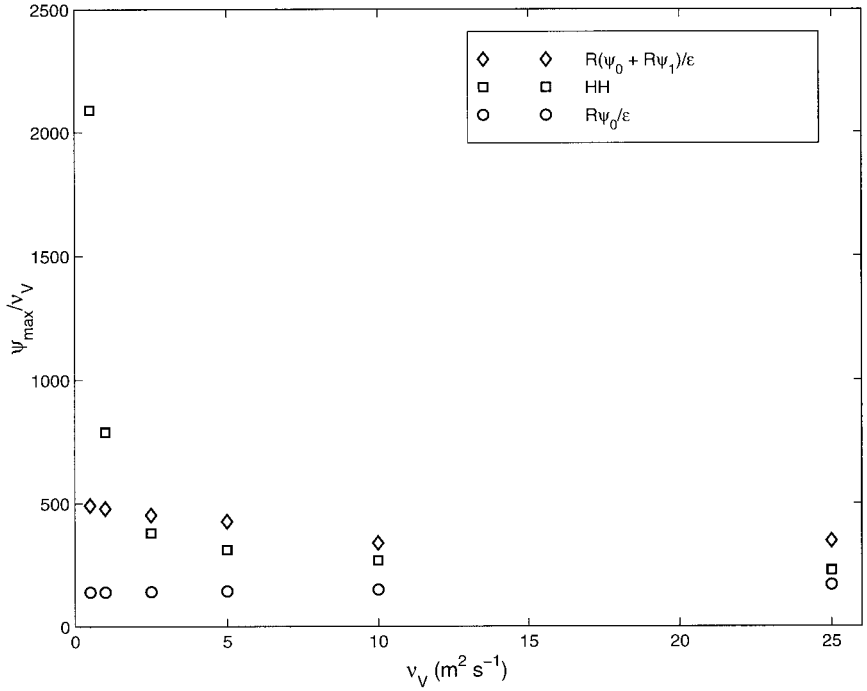

FIG. 11. The ratio of streamfunction maximum to vertical viscosity, as a function of ν_V, for the sequence shown in Fig. 4 of HH. All the other parameters have the values listed in (4.1). The diamonds mark the maxima of $R(\psi_0 + R\psi_1)/\epsilon$ obtained solving (3.11), while the circles show the maxima of $R\psi_0/\epsilon$. The numerical results for $\psi_{\max}/\nu_V$ published in HH are marked by squares. While the maxima obtained solving (3.11) are almost independent of viscosity for all values of ν_V, $\psi_{\max}/\nu_V$ computed by HH exhibit a sudden increase for the two smallest values of ν_V, indicating that a qualitative change in the dynamical balance takes place for these values of viscosity.

In the range of parameters where our results agree with the direct computations of HH, the potential temperature is laterally homogenized within the cells, and the advection of the stable stratification imposed by the radiative–convective equilibrium is essential for the determination of the scale of the meridional cell, while the angular momentum balance plays a marginal role. Thus, the Hadley circulation expands linearly with the equatorial baroclinic radius of deformation, in agreement with Schneider and Lindzen (1976) and Schneider (1977). This scaling result departs from the conclusions drawn by HH.

When stratification is absent or the surface drag is much weaker than that used by HH, both angular momentum and potential temperature are homogenized inside the Hadley cells. This regime approaches the HH ideal of the axially symmetric meridional circulation, where conservation of angular momentum is important. In this regime, surface easterlies are found at the equator, even for a heating distribution that centered at the equator.

Acknowledgments. I am especially indebted to Piero Malguzzi for illuminating discussions and for providing me with his Newton–Keller subroutines. Numerous conversations with Bill Young are gratefully acknowledged. Ed Schneider and an anonymous referee are thanked for their constructive criticism. Funding for this research is provided by the Department of Energy through its CHAMMP Program (DOE DEFG03 93ER61690).

APPENDIX A

The Vertical Structure of the Meridional Streamfunction

In this section exact and approximate solutions for the vertical structure of the meridional circulation, ψ_0 in section 3, are given. This amounts to solving the ordinary differential equation (3.8), repeated here for convenience,

$$E^2c^2\phi_{zzzz} - y(\mathcal{M}^2)_y\phi = c^4, \tag{A.1}$$

with boundary conditions $\phi = \phi_{zz} = 0$ at $z = 0, 1$. The lowest order approximation to the streamfunction ψ_0 is then given by

$$\psi_0 = -\Theta_y\phi. \tag{A.2}$$

The exact solution of (A.1) is

$$\phi = -\frac{c^4}{y(\mathcal{M}^2)_y}[1 - A\cos\eta(2z-1)\cosh\eta(2z-1) - B\sin\eta(2z-1)\sinh\eta(2z-1)],$$

$$A \equiv \frac{\cos\eta\cosh\eta}{\cos^2\eta + \sinh^2\eta}, \qquad B \equiv \frac{\sin\eta\sinh\eta}{\cos^2\eta + \sinh^2\eta},$$

$$\eta \equiv \left[\frac{-y(\mathcal{M}^2)_y}{64E^2c^2}\right]^{1/4}. \tag{A.3}$$

The solution (A.3) parallels that of Charney (1973): the streamfunction is independent of z except in the top and bottom Ekman layers of thickness η^{-1}. Here, however, η depends on the surface angular momentum $\mathcal{M}$ and its gradient, while in Charney's linear solution $\mathcal{M}$ is replaced by its planetary value, c^2. Thus the thickness of the Ekman layer becomes infinite not just at the equator, but in the whole region of angular momentum homogenization.

Expression (A.3) is so complicated that the integrals needed in (3.11) were obtained with the aid of a symbolic manipulation software (MAPLE). Alternatively, the following series expansion, suggested by W. R. Young (1997, personal communication), converges very quickly:

$$\phi = \frac{4c^2}{\pi}\sum_{n=0}^{\infty}\frac{\sin(2n+1)\pi z}{(2n+1)[E^2(2n+1)^4\pi^4 - c^{-2}y(\mathcal{M}^2)_y]}. \tag{A.4}$$

This series clearly shows that (A.1) has no solution wherever

$$c^{-2}y(\mathcal{M}^2)_y = E^2(2n+1)^4\pi^4.$$

Appendix B shows that the pole at $n = 0$ in (A.4) coincides with the onset of symmetric instability in the original Boussinesq system (2.13). Each successive pole in (A.4) corresponds to the excitation of another unstable mode.

With the series (A.4) the integrals in (3.11) are well approximated by just keeping the first term in (A.4) and

$$\int_0^1 \phi\,dz \approx \frac{8c^2}{\pi^2[E^2\pi^4 - c^{-2}y(\mathcal{M}^2)_y]},$$

$$\int_0^1 \phi^2\,dz \approx \frac{8c^4}{\pi^2[E^2\pi^4 - c^{-2}y(\mathcal{M}^2)_y]^2},$$

$$\int_0^1 z(1-z)\phi\,dz \approx \frac{16c^2}{\pi^4[E^2\pi^4 - c^{-2}y(\mathcal{M}^2)_y]}. \tag{A.5}$$

In the numerical solutions presented in sections 4 and 5, the exact expression (A.3) was used to evaluate the integrals in (3.11). The approximations in (A.5) are useful in the analytic calculations presented in sections 4 and 5.

APPENDIX B

Symmetric Instability in the Presence of Viscosity

In this appendix we examine the conditions for which a steady solution of (2.13) in the form

$$M = \mathcal{M}(y), \qquad \psi = 0, \qquad \theta = 0, \tag{B.1}$$

is linearly stable. We restrict the analysis to the case where $\mu = 0$ in (2.13) and $\gamma = 0$ in (2.14). Infinitesimal perturbations, M' and ψ', of the basic state (B.1) satisfy the system

$$R(M'_t - \mathcal{M}_y\psi'_z) = M'_{zz},$$

$$R^2E^2\psi'_{zzt} - 2yc^{-2}\mathcal{M}M'_z = RE^2\psi'_{zzzz} \quad \text{(B.2)}$$

with boundary conditions $\psi' = \psi'_{zz} = M'_z = 0$ at $z = 0$ and $z = 1$.

Without any temperature structure in the basic state, temperature perturbations decay in time regardless of flow disturbances and are thus omitted in the vorticity equation. We seek perturbations that are exponentially growing in time:

$$\psi' = A(y, z)\exp(st),$$
$$M' = B(y, z)\exp(st). \quad \text{(B.3)}$$

The system (B.2) can be reduced to the single equation in B:

$$(R^2E^2s^2 - 2yc^{-2}\mathcal{M}\mathcal{M}_y)B_z - 2RE_s^2B_{zzz} + E^2B_{zzzzz} = 0 \quad \text{(B.4)}$$

subject to the boundary conditions $B_z = B_{zzz} = 0$ at $z = 0$ and $z = 1$. Notice that B is only differentiated with respect to z, and its dependence on y is parametric. In this simple case, where there is no basic stratification and no vertical shear, the growth rate s can be a function of latitude y. Nontrivial solutions

$$B = b\cos n\pi z,$$
$$A = (Rs + n^2\pi^2)(Rn\pi\mathcal{M}_y)^{-1}b\sin n\pi z \quad \text{(B.5)}$$

are obtained when the growth rate satisfies the dispersion relation

$$R^2E^2s^2 + 2RE^2n^2\pi^2s + E^2n^4\pi^4 - yc^{-2}(\mathcal{M}^2)_y = 0. \quad \text{(B.6)}$$

The roots of (B.6) are

$$REs = -En^2\pi^2 \pm \sqrt{yc^{-2}(\mathcal{M}^2)_y} \quad \text{(B.7)}$$

and one of the roots becomes positive wherever

$$yc^{-2}(\mathcal{M}^2)_y > E^2n^4\pi^4. \quad \text{(B.8)}$$

Thus, the threshold for which at least one vertical mode becomes unstable to symmetric disturbances is obtained by setting $n = 1$ in (B.8).

APPENDIX C

The $O(R)$ Correction to the Meridional Streamfunction ψ_1

In this section the first correction to the leading order field for the streamfunction is calculated. The same procedure can be used to calculate the $O(R^2)$ corrections to the angular momentum and temperature fields, M_2 and θ_2 respectively.

The vorticity equation at $O(R^2)$ is

$$E^2[c^{-2}\psi_{0zzt} + J(\psi_0, c^{-2}\psi_{0zz})] - 2yc^{-4}(M_1M_{1z} + \mathcal{M}M_{2z}) = \theta_{1y} + E^2c^{-2}\psi_{1zzzz}. \quad \text{(C.1)}$$

The fields θ_1 and M_1 are given in terms of the "master" fields $\mathcal{M}$ and Θ in (3.7), while the field M_2 is obtained from (3.10) after using (3.11) to eliminate the term $\mathcal{M}_{t_1}$; that is,

$$\gamma_2(c^2 - \mathcal{M}) + \left[\mathcal{M}_y\Theta_y^2\int_0^1\phi^2\,dz - \mathcal{M}_y\Theta_y^2\phi^2\right]_y + \left[\Theta_y\phi\left(\Theta_y\mathcal{M}_y\int_0^z\phi\,d\hat{z}\right)_y\right]_z - \psi_{1z}\mathcal{M}_y = M_{2zz}, \quad \text{(C.2)}$$

where (3.7a,b) have been used to calculate M_1 and ψ_0. Integrating (C.2) once in z and using the boundary condition $M_{2z}|_{z=0} = \gamma_2(\mathcal{M} - c^2)$ we find

$$M_{2z} = \gamma_2(c^2 - \mathcal{M})(z - 1) + \left[z\mathcal{M}_y\Theta_y^2\int_0^1\phi^2\,dz - \mathcal{M}_y\Theta_y^2\int_0^z\phi^2\,d\hat{z}\right]_y + \Theta_y\phi\left(\Theta_y\mathcal{M}_y\int_0^z\phi\,d\hat{z}\right)_y - \psi_1\mathcal{M}_y. \quad \text{(C.3)}$$

Substituting (C.3) and (3.7a, b) into (C.1) one obtains, in steady state,

$$E^2c^4J(\Theta_y\phi, c^{-2}\Theta_y\phi_{zz}) - 2y(\Theta_y\mathcal{M}_y)^2\phi\int_0^z\phi\,d\hat{z} - c^4\left[\Theta_y^2\left(\int_0^1 z\phi\,dz - \int_z^1\phi\,d\hat{z}\right)\right]_y$$
$$-2y\mathcal{M}\left[\gamma_2(c^2 - \mathcal{M})(z - 1) + \left(z\mathcal{M}_y\Theta_y^2\int_0^1\phi^2\,dz - \mathcal{M}_y\Theta_y^2\int_0^z\phi^2\,d\hat{z}\right)_y + \Theta_y\phi\left(\Theta_y\mathcal{M}_y\int_0^z\phi\,d\hat{z}\right)_y\right]$$
$$= E^2c^2\psi_{1zzzz} - y(\mathcal{M}^2)_y\psi_1. \quad \text{(C.4)}$$

At this order the boundary conditions on ψ_1 at the top and the bottom are no normal flow and no stress so that (C.4) is the same type of equation as (3.8) except that the right-hand side depends on z as well as y. In the figures shown in this work, (C.4) is solved numerically using a rapidly converging series expansion of the type given in (A.4).

The essential point is that, in the limit of small Ekman number E, ψ_1 is independent of E outside of the thin top and bottom boundary layers, as is the case for ψ_0 and ϕ.

REFERENCES

Bretherton, F. P., and J. S. Turner, 1968: On the mixing of angular momentum in a stirred rotating fluid. *J. Fluid Mech.*, **32,** 449–464.

Charney, J. G., 1973: Planetary fluid dynamics. *Dynamic Meterology*, P. Morel, Ed., Reidel, 97–351.

Fang, M., and K. K. Tung, 1994: Solution to the Charney problem of viscous symmetric circulation. *J. Atmos. Sci.*, **51,** 1261–1272.

——, and ——, 1996: A simple model of nonlinear Hadley circulation with an ITCZ: Analytic and numerical solutions. *J. Atmos. Sci.*, **53,** 1241–1261.

Held, I. M., and A. Y. Hou, 1980: Nonlinear axially symmetric circulation in a nearly inviscid atmosphere. *J. Atmos. Sci.*, **37,** 515–533.

Lindzen, R. S., 1990: *Dynamics in Atmospheric Physics*. Cambridge University Press, 310 pp.

——, and H. Y. Hou, 1988: Hadley circulation for zonally averaged heating centered off the equator. *J. Atmos. Sci.*, **45,** 2416–2427.

Read, P. L., 1986: Super-rotation and diffusion of axial angular momentum: II. A review of quasi-axisymmetric models of planetary atmospheres. *Quart. J. Roy. Meteor. Soc.*, **112,** 253–272.

Satoh, M., 1994: Hadley circulations in radiative convective equilibrium in an axially symmetric atmosphere. *J. Atmos. Sci.*, **51,** 1947–1968.

Schneider, E. K., 1977: Axially symmetric steady-state models of the basic state for instability and climate studies. Part II. Nonlinear calculations. *J. Atmos. Sci.*, **34,** 280–296.

——, and R. S. Lindzen, 1976: The influence of stable stratification on the thermally driven tropical boundary layer. *J. Atmos. Sci.*, **33,** 1301–1307.